Trajectories of square lattice staircase polygons

EJ Janse van Rensburg

Department of Mathematics and Statistics, York University, Toronto, Ontario M3J 1P3, Canada

E-mail: rensburg@yorku.ca

27 April 2023

Abstract. The distribution of monomers in a coating of grafted and adsorbing polymers is modelled using a grafted staircase polygon in the square lattice. The adsorbing staircase polygon consists of a bottom and a top lattice path (branches) and the asymptotic probability density that vertices in the lattice are occupied by these paths is determined. This is a model consisting of two linear polymers grafted to a hard wall in a coating. The probability that either the bottom, or the top, path of a staircase polygon passes through a lattice site with coordinates $(\lfloor \epsilon n \rfloor, \lfloor \delta \sqrt{n} \rfloor)$, for $0 < \epsilon < 1$ and $\delta \geq 0$, is determined asymptotically as $n \to \infty$. This gives the probability density of vertices in the staircase polygon in the scaling limit (as $n \to \infty$):

$$\mathbb{P}_r^{f,(both)}(\epsilon,\delta) = \frac{\delta^2(15\,\epsilon^2(1-\epsilon)^2 - 12\,\delta^2\epsilon(1-\epsilon) + 4\,\delta^4)}{3\sqrt{\pi\,\epsilon^7(1-\epsilon)^7}}\,e^{-\delta^2/\epsilon(1-\epsilon)}.$$

The densities of other cases, grafted and adsorbed, and at the adsorption critical point (or special point), are also determined. In these cases the most likely and mean trajectories of the paths are determined. The results show that low density regions in the distribution induces entropic forces on test particles which confine them next to the hard wall, or between branches of the staircase polygon. These results give qualitative mechanisms for the stabilisation of a drug particle confined to a polymer coating in a drug delivery system such as a drug-eluding stent covered by a grafted polymer.

Keywords: Staircase polygons, exact probability densities, directed polymers, directed paths, adsorbed polymers

PACS numbers: 82.35.-x, 36.20.-r

AMS classification scheme numbers: 82B41,82B23

1. Introduction

Polymer coatings on surfaces or on suspended colloid particles have applications in medical and industrial systems. For example, there are important uses in targeted drug delivery systems [17,18,23], including nanoparticle-polymer systems [24,25]. Polymer coatings on drug-eluding stents are now widely used to deliver a drug over a period time [7] at the location of the stent. In other examples, the steric stabilisation of colloid dispersions by coating particles with a polymer are important in a variety

of applications [8, 20]. In this case the colloid particles are coated with a polymer and, if they approach each other, experience repulsive forces due to the reduction in configurational entropy of the polymers between them. In nano-particle systems and drug eluding stents a particle is suspended in a polymer coating and it may diffuse from the coating over time, or be released as the coating degrades. Copolymers are frequently used in these systems, and in figure 1 (left panel) a schematic diagram of a 2-block copolymer grafted to a surface is shown. The copolymer coils near the surface to form a coating into which a drug absorbs to be released later at a target site.

In these applications the properties of the polymeric coating plays an important role. A hydrophylic coating has polymer coils that form a thicker and less dense layer, while a hydrophobic coating results in a thinner and denser layer. Both thinner and thicker coatings have their applications, and the density distribution of the layer (for example, less dense towards the wall, more dense away from it) are relevent.

In reference [15] a directed path model of a grafted linear polymer in a polymer coating was examined. It was shown there that the entropic repulsion between the hard wall and the directed path creates a low density region next to the wall, providing a metastable location for absorbed particles next to the wall. However, this region disappears when the path adsorbs on the wall, indicating that a grafted polymer (rather than an adsorbed polymer) would be more efficient in retaining particles in the coating.

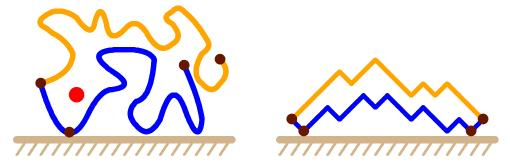


Figure 1: (Left) A schematic diagram of a linear polymers in a coating confining a particle. In this diagram a 2-block copolymer is shown, with one of the blocks grafted to the wall. Steric repulsions between the two blocks and the hard wall create low density regions in the coating. One block may adsorb on the surface. (Right) A staircase polygon model of a grafted 2-block ring copolymer. The bottom block is grafted at both its endpoints to the wall (and may adsorb on the wall), while the top block is screened from the surface by the bottom block. Each of the blocks in the staircase polygon is a directed path giving North-East or South-East in the square lattice.

In this paper a more elaborate directed path model of polymers in a polymer coating is examined. In figure 1 (left panel) a schematic drawing of a 2-block copolymer, with one block grafted to a hard wall, is shown. The two blocks avoid each other and the wall, and if they approach each other of the wall, then a reduction in configurational entropy induces mutually repulsive forces between them. If the polymer is a 2-block ring copolymer, then it can be modelled by a grafted staircase polygon shown in the right panel of figure 1. Two directed lattice paths, starting in the same vertex, giving North-East (NE) and South-East (SE) steps and avoiding each

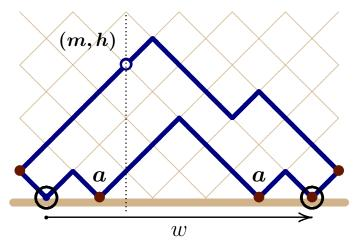


Figure 2: A staircase polygon grafted at the origin and at the end of its bottom path. The width w of the polygon is equal to the length of its bottom path minus 2. Each return of the bottom path to the hard wall, except the origin and the last grafted vertex, is weighted by a. The top path passes through the vertex with coordinates (m, h) and by calculating the probability of events like this, the probability density of the polygon is obtained in the limit as its length increases to infinity. The width of the polygon is the distance from the origin to the penultimate vertex in the bottom path, or the number of steps between the origin and the penultimate vertex in the bottom path.

other, end in the same vertex to form a lattice polygon. The bottom directed path is one block, and it is grafted to the wall at both endpoints, and may also adsorb on the wall if there is a strong attractive force between the wall and the vertices in the path. The top path is the second block, and it is screened from the wall by the bottom path. More generally, this is also a two dimensional model of two interacting linear polymers grafted to the wall, with one adsorbing onto the wall.

There is an extensive literature in the physical sciences on directed path models of adsorbing and grafted polymers [6,9,10,21,26]. These models are exactly solvable, and have proven particularly usefull as a tool to quantify the entropy of a directed linear polymer and exposing the general scaling and phase behaviour in linear polymers. The simplest models are Dyck paths [1,3,5,11-13,16,22] and these are related to staircase polygons [4,16,19].

1.1. Adsorbing staircase polygon models

The length of a directed lattice path giving NE and SE steps in the square lattice \mathbb{L} is its number of steps. Since the path always steps one unit per step in the East direction, the length of the path is also its width. The length of a staircase polygon is the sum of the lengths of its bottom and top paths (see figure 2), or twice the length of either its bottom or top path. A staircase polygon is grafted at both its endpoints if the second and penultimate vertices in the bottom path are fixed in the hard wall. The width of a grafted staircase polygon is equal to the length of its bottom walk minus 2, as illustrated in figure 2. If returns of the bottom path to the wall (except for the grafted vertices) are weighted by a Boltzmann factor $a = e^{-\mathcal{E}/kT}$, then the

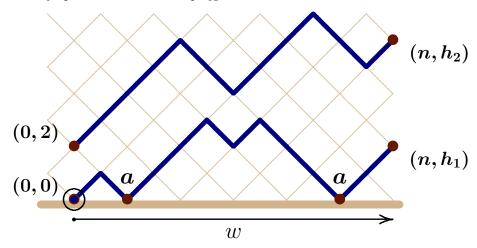


Figure 3: Two osculating paths from vertices with coordinates (0,0) and (0,2) in the square lattice, giving NE and SE steps, and ending in vertices with coordinates (n,h_1) and (n,h_2) , and heights $h_1 < h_2$. Returns of the bottom path to the hard wall (the x-axis) are weighted by the parameter a. The width w of the paths is indicated and is the number of steps in bottom path. This is also the half-length of the pair of paths.

staircase polygon is *adsorbing* and \mathcal{E} is a binding energy of a vertex to the hard wall, T is the absolute temperature and k is Boltzmann's constant.

The left-most and right-most two steps in a staircase polygon have fixed orientation and may be removed without affecting the combinatorial properties of the remaining paths. This gives two directed paths (a bottom path and a top path). More generally, these paths may be allowed to end in vertices which are farther apart, so that they cannot be reconnected to form a staircase polygon. This is illustrated in figure 3. Since the paths avoid one another, but may approach closely to "bounce" off each other, they are also called *osculating paths*; see for example reference [2].

Consider vertices (n, m) of even parity (that is, n + m is even) in \mathbb{L} . The bottom directed path in figure 3 starts in (0,0), has length n, and ends in (n,h_1) , while the top path starts in (0,2) and ends in (n,h_2) . The width of the pair of paths is w = n. Two steps can be prepended to the left in figure 3, and if $h_2 = h_1 + 2$, then another two steps can be appended to the right to join the two paths into a staircase polygon. More generally, if only the two steps are prepended to the left in figure 3, then the two paths is a directed path model of a 2-star copolymer (figure 1(left)), with its bottom arm adsorbing in a hard wall.

If $h_1 = 0$ and $h_2 = 2$ in figure 3, and steps are prepended to the left and appended on the right, the paths become a staircase polygon grafted at both endpoints (so that the second and penultimate vertices in the bottom path are grafted to the hard wall). This staircase polygon have total length 2n + 4 and width w = n. Returns of the bottom path to the hard wall, except at the grafted vertices, are weighted by a. If a = 1, then the bottom path is said to be free, and the paths or staircase polygon is in a desorbed or free phase [16]. For a > 2 the bottom path is adsorbed on the wall, and the model is in an adsorbed phase. These phases are separated by the adsorption critical point $a_c = 2$ (the special point); for more results about the phase diagram of adsorbing staircase polygons, see reference [14].

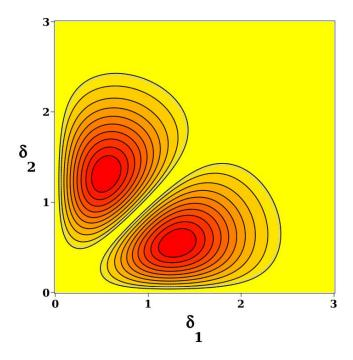


Figure 4: Contourplot of $|\mathbb{P}_r^{(2)}(1,\delta_1,\delta_2)|$ on the $\delta_1\delta_2$ -plane. Low values are in light shades, and high values are in darker shades. This shows that paths with endpoints at $(\delta_1,\delta_2)\approx (0.5412,1.3066)$ dominate the partition function in the limit as $n\to\infty$, so that the most likely heights of the endpoints are approximately $h_1\approx 0.5412\sqrt{n}$ and $h_2\approx 1.3066\sqrt{n}$.

1.2. Probability densities of grafted staircase polygons

The paths in figures 2 and 3 have length n and are ballistic in the horizontal direction so that the natural horizontal length scale is O(n). In the vertical direction the paths are random walks, with vertical length scale $O(\sqrt{n})$. By rescaling the lattice an asymptotic probability distribution for paths passing through specific lattice sites in \mathbb{Z}^2 can be determined. Though not rigorous, this distribution converges in the limit as $n \to \infty$ to the (exact) probability density of the paths passing through points in \mathbb{R}^2 . This is the *scaling limit* of the model. The calculation relies on (non-rigorous) asymptotic estimates of the finite size probability distribution.

In section 2 the model of osculating paths in figure 3 is considered in the free phase (with a=1). The number of pairs of paths of width n and heights $h_1=j-\ell$ and $h_2=j+\ell+2$ is given by (see for example reference [14] equation (5.172))

$$U_n(j,\ell) = \frac{(j+2)(\ell+1)(j-\ell+1)(j+\ell+3)}{(n+1)(n+2)(n+3)^2} \binom{n+3}{(n+j-\ell)/2+2} \binom{n+3}{(n+j+\ell)/2+3}, \quad (1)$$

where j and ℓ have the same parity as n and $j \geq \ell$. By putting $j = \ell = 0$ and "capping" the left starting points the number of staircase polygon of length 2n + 4, grafted at (0,0) and (n,0), is given by $U_n(0,0)$.

Define $V_n(h_1, h_2) \equiv U_n(j, \ell)$ (with $h_1 = j - \ell$ and $h_2 = j + \ell + 2$). A probability

distribution can be determined from $U_n(j,\ell)$ for the probability that the two paths end in heights $h_1 = \lfloor \delta_1 \sqrt{n} \rfloor$ and $h_2 = \lfloor \delta_2 \sqrt{n} \rfloor$. This is obtained from equation (1) by substituting $h_1 = j - \ell = \lfloor \delta_1 \sqrt{n} \rfloor$ and $h_2 = j + \ell + 2 = \lfloor \delta_2 \sqrt{n} \rfloor$, and then normalising. To leading order,

$$U_{\lfloor \sigma n \rfloor} = V_{\lfloor \sigma n \rfloor}(\lfloor \delta_1 \sqrt{n} \rfloor, \lfloor \delta_2 \sqrt{n} \rfloor) \equiv V_{\lfloor \sigma n \rfloor}(\delta_1, \delta_2) \simeq \frac{\delta_1 \delta_2(\delta_2^2 - \delta_1^2)}{\pi n^3 \sigma^5} 16^{n\sigma + 1} e^{-(\delta_1^2 + \delta_2^2)/\sigma},$$
(2)

where the arguments of $U_{\lfloor \sigma n \rfloor}(j,\ell)$ are surpressed for clarity. The normalising factor N_u for U_n is obtained by integrating it for $0 < \delta_1 < \delta_2 < \infty$. This gives

$$N_u = \int_0^\infty \int_{\delta_1}^\infty U_n \, d\delta_2 \, d\delta_1 = \frac{16^{\sigma n + 1/4}}{\pi n^3 \sigma^2}.$$
 (3)

Dividing $U_{\lfloor \sigma n \rfloor}/N_u$ gives the asymptotic probability density which is independent of n and therefore is the exact probability probability density in the scaling limit:

$$\mathbb{P}_{r}^{(2)}(\sigma, \delta_{1}, \delta_{2}) = \frac{8 \,\delta_{1} \delta_{2}(\delta_{2}^{2} - \delta_{1}^{2})}{\sigma^{3}} \,e^{-(\delta_{1}^{2} + \delta_{2}^{2})/\sigma}, \quad \text{for } 0 \le \delta_{1} \le \delta_{2} < \infty. \tag{4}$$

Details are given in section 2.

Putting $\sigma = 1$ and plotting the absolute value $|\mathbb{P}_r^{(2)}(1, \delta_1, \delta_2)|$ in the $\delta_1 \delta_2$ -plane gives figure 4. Notice that this is the asymptotic probability density that the endpoints of paths of length n end in the vertices $(n, \lfloor \delta_1 \sqrt{n} \rfloor)$ (bottom path), and $(n, \lfloor \delta_2 \sqrt{n} \rfloor)$ (top path) in the scaling limit. By determining the maxima in the plot, the most likely heights of the endpoints are obtained with $\delta_1 = \sqrt{\sqrt{2} - 1}/\sqrt{8} \approx 0.5412$ and $\delta_2 = \sqrt{\sqrt{2} + 2}/\sqrt{2} \approx 1.3066$.

The asymptotic probability that the staircase polygon passes through a vertex $(\lfloor \epsilon n \rfloor, \lfloor \delta \sqrt{n} \rfloor)$ can be determined from equation (1), and its asymptotic form $V_{\lfloor \sigma n \rfloor}(\delta_1, \delta_2)$ in equation (2). In figure 5 a grafted staircase polygon passing through the points $(\lfloor \epsilon n \rfloor, \lfloor \delta_1 \sqrt{n} \rfloor)$ (in its bottom branch) and $(\lfloor \epsilon n \rfloor, \lfloor \delta_2 \sqrt{n} \rfloor)$ (in its top branch) is illustrated. The vertical dotted line splits the polygon into two parts, one part a pair of osculating paths of width $\lfloor \epsilon n \rfloor$ from the left, and the other a pair of osculating paths of width $\lfloor \epsilon n \rfloor$ from the right.

The asymptotic number of pairs of osculating paths are given in equation (2). This gives the asymptotic number of staircase polygons in figure 5 as approximately

$$V_{\lfloor \epsilon n \rfloor} \left(\lfloor \delta_1 \sqrt{n} \rfloor, \lfloor \delta_2 \sqrt{n} \rfloor \right) \times V_{\lfloor (1 - \epsilon) n \rfloor} \left(\lfloor \delta_1 \sqrt{n} \rfloor, \lfloor \delta_2 \sqrt{n} \rfloor \right). \tag{5}$$

By normalising this expression, the probability density that the bottom path passes through the vertex with coordinates $(\lfloor \epsilon n \rfloor, \lfloor \delta_1 \sqrt{n} \rfloor)$, and the top path passes through $(\lfloor \epsilon n \rfloor, \lfloor \delta_2 \sqrt{n} \rfloor)$, is obtained in the scaling limit. This is given by

$$\mathbb{P}_r^f(\epsilon, \delta_1, \delta_2) = \frac{32}{3} \frac{(\delta_2^2 - \delta_1^2)^2 \, \delta_1^2 \delta_2^2}{\pi \, \epsilon^5 \, (1 - \epsilon)^5} \, e^{-(\delta_1^2 + \delta_2^2)/\epsilon (1 - \epsilon)}. \tag{6}$$

Integrating $\mathbb{P}_r^f(\epsilon, \delta_1, \delta_2)$ for $0 < \delta_2 < \infty$ and putting $\delta_1 = \delta$ gives the probability density

$$\mathbb{P}_r^{f,(both)}(\epsilon,\delta) = \int_0^\infty \mathbb{P}_r^{(2)}(\epsilon,\delta,\delta_2) \, d\delta_2 \tag{7}$$

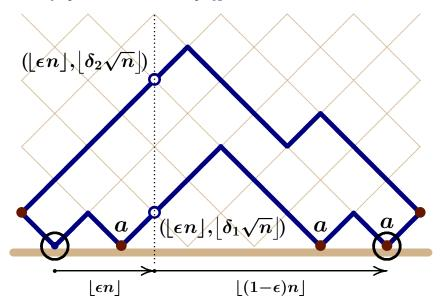


Figure 5: A staircase polygon grafted at the origin and at the end of its bottom directed path. By cutting the path along the vertical dotted line, two pairs of directed paths, one pair from the left, and the other from the right, are obtained. The probability that the bottom path passes through the vertex with coordinates ($\lfloor \epsilon n \rfloor$, $\lfloor \delta_1 n \rfloor$), and the top path passes through the vertex with coordinates ($\lfloor \epsilon n \rfloor$, $\lfloor \delta_2 n \rfloor$) is obtained by approximating the number of pairs of paths passing through these vertices.

that either the bottom path, or the top path, passes through points (ϵ, δ) in the infinite rectangle $S = [0, 1] \times [0, \infty) \subseteq \mathbb{R}^2$. Simplifying the result gives

$$\mathbb{P}_r^{f,(both)}(\epsilon,\delta) = \frac{\delta^2(15\,\epsilon^2(1-\epsilon)^2 - 12\,\delta^2\epsilon(1-\epsilon) + 4\,\delta^4)}{3\,\sqrt{\pi}\,\sqrt{\epsilon^7(1-\epsilon)^7}}\,e^{-\delta^2/\epsilon(1-\epsilon)}.\tag{8}$$

A contourplot of this density is plotted in figure 6. Notice that there are low density regions next to the hard wall and between the trajectories of the bottom and top paths. This shows that the entropic repulsion between the paths, and between the bottom path and the wall, create low density regions in this model of polymer coatings that particles can occupy in a metastable state before they are released when overcoming the entropic barriers.

The domain of the probability density $\mathbb{P}_r^{f,(both)}(\epsilon,\delta)$ can be extended from S to all of \mathbb{R}^2 by defining $\mathbb{P}_r^{f,(both)}(\epsilon,\delta)=0$ if $(\epsilon,\delta) \notin S$. Define $R=(x_1,x_2)\times(y_1,y_2)$ to be an open rectangle in \mathbb{R}^2 , and suppose that \overline{R} is the closure of R. Define the set function ν by

$$\nu R = \nu \overline{R} = \int_{-\infty}^{\infty} \int_{-\infty}^{\infty} \mathbb{P}_r^{f,(both)}(\epsilon, \delta) \, d\delta \, d\epsilon. \tag{9}$$

Then ν is a set-function on the semi-algebra of rectangles in \mathbb{R}^2 , and it is additive on unions of disjoint rectangles. It follows that $\nu(R \cap S) = \nu R$, and on subsets of the $\epsilon \delta$ -plane ν extends to an outer measure. On the σ -algebra of plane measure sets ν is

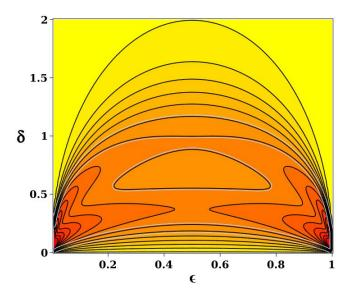


Figure 6: Contourplot of the density $\mathbb{P}_r^f(\epsilon, \delta)$ of grafted staircase polygons in the scaling limit. Lighter regions have low densities. The plot shows low densities adjacent to the hard wall, and also a region of relative low density between the top and bottom paths.

a measure, and if E is a plane measurable set with respect to plane measure λ , then

$$\nu E = \int_{E} \mathbb{P}_{r}^{f,(both)}(\epsilon, \delta) d\lambda. \tag{10}$$

The Radon-Nikodym derivative of ν with respect to λ is $\frac{d\nu}{d\lambda} = \mathbb{P}_r^{f,(both)}(\epsilon, \delta)$ at the point $(\epsilon, \delta) \in \mathbb{R}^2$. Since $\nu \mathbb{R}^2 = 1$, it is a probability measure on λ -measure sets, and νE is the probability that paths from the origin (0,0) to (1,0) pass through E.

1.3. Organization of the paper

In section 2 some details of the derivation of equation (2) are given. The most probable trajectories of the bottom and top paths are determined, as well as the probability densities of the bottom path, or the top path, passing through a point, and their most likely trajectories.

In section 3 the cases of adsorbed staircase polygons are considered. The situation is more complicated and some details are given in the Appendix. In this case the bottom path is adsorbed on the wall, changing the density of the model. The density at the critical point $a_c = 2$ (the *special point*) is also distinct from either the densities in the free or in the adsorbed phase, and this is presented in section 4.

A final discussion of the results, as well as the most likely and mean trajectories and entropic forces, are given in section 5.

2. The densities of paths in the free phase

2.1. The density of both paths in the free phase

In this section more details of the derivation of equations (2) and (4) are given. Substituting and approximating $j-\ell=h_1=|\delta_1\sqrt{n}|\simeq\delta_1\sqrt{n},\ j+\ell+2=h_2=$ $|\delta_2\sqrt{n}| \simeq \delta_2\sqrt{n}$ and replacing and then approximating $n \to |\sigma n| \simeq \sigma n$ in equation (2) gives (where the arguments of $V_{|\sigma n|}$ are left away for simplicity)

$$V_{\lfloor \sigma n \rfloor} = \frac{\left((\delta_2 - \delta_1) \sqrt{n} \right) \left((\delta_1 + \delta_2) \sqrt{n} + 1 \right) \left(2 \, \delta_1 \sqrt{n} + 1 \right) \left(2 \, \delta_2 \sqrt{n} + 1 \right)}{\left(2 \, n \sigma + 1 \right) \left(2 \, n \sigma + 2 \right) \left(2 \, n \sigma + 3 \right)^2} \begin{pmatrix} 2 \, n \sigma + 3 \\ n \sigma + \delta_1 \sqrt{n} + 2 \end{pmatrix} \begin{pmatrix} 2 \, n \sigma + 3 \\ n \sigma + \delta_2 \sqrt{n} + 2 \end{pmatrix}.$$

Convert the binomial coefficients into factorials. Using the Stirling approximation in equation (77) to approximate the factorials and simplifying the result shows that, to leading order,

$$V_{[\sigma n]} \simeq \frac{3}{2\pi} \frac{\sqrt{n} (\delta_2 - \delta_1) a_0 a_1 a_3 a_4^{a_1 a_1} a_5 a_{11}^{a_{11}}}{\sqrt{a_7 a_8 a_9 a_{10}} a_6^{a_1 7} a_{12}^{a_1 2} a_{13}^{a_2} a_{14} a_{15}},$$
(11)

where

where
$$a_0 = \delta_1 \sqrt{n} + \delta_2 \sqrt{n} + 1, \qquad a_1 = 2 \, \delta_1 \sqrt{n} + 1, \qquad a_2 = n\sigma - \delta_2 \sqrt{n} + 1$$

$$a_3 = 2 \, \delta_2 \sqrt{n} + 1, \qquad a_4 = 2 \, n\sigma + 3, \qquad a_5 = 12 \, n\sigma + 19,$$

$$a_6 = n\sigma + \delta_1 \sqrt{n} + 2, \qquad a_7 = 6 \, n\sigma + 6 \, \delta_1 \sqrt{n} + 13, \qquad a_8 = 6 \, n\sigma - 6 \, \delta_1 \sqrt{n} + 7,$$

$$a_9 = 6 \, n\sigma + 6 \, \delta_2 \sqrt{n} + 13, \qquad a_{10} = 6 \, n\sigma - 6 \, \delta_2 \sqrt{n} + 7, \qquad a_{11} = n\sigma - \delta_1 \sqrt{n} + 1,$$

$$a_{12} = n\sigma + \delta_2 \sqrt{n} + 2, \qquad a_{13} = n\sigma - \delta_2 \sqrt{n} + 1, \qquad a_{14} = 2 \, n\sigma + 1,$$

$$a_{15} = n\sigma + 1, \qquad a_{16} = 4 \, n\sigma + 4, \qquad a_{17} = n\sigma + \delta_1 \sqrt{n} + 2,$$

$$a_{18} = \delta_1 \sqrt{n} - n\sigma - 1, \qquad a_{19} = n\sigma + \delta_2 \sqrt{n} + 2.$$

Taking the logarithm of equation (11) and expanding, and then expanding the resulting terms each asymptotically while discarding terms decaying with n give, after exponentiating and simplifying the result, equation (2), and, after normalisation, the probability density in equation (4).

2.1.1. The most likely and mean trajectories in the free phase: The density plot in figure 6 shows that there are most likely trajectories for the bottom and top paths. These may be assumed to run along the peaks in the plot so that they are "modal paths" from (0,0) to (1,0). Solving for local minima and maxima for fixed values of $\epsilon \in (0,1)$ in equation (6) shows that the extreme values of δ as a function of ϵ is given by solutions of the polynomial

$$8\delta^{6} - 48\delta^{4}\epsilon(1-\epsilon) + 78\delta^{2}\epsilon^{2}(1-\epsilon)^{2} - 30\epsilon^{3}(1-\epsilon)^{3} = 0.$$
 (12)

Solving for δ gives δ_M , the most likely trajectories of the paths, and also its (locally)

least likely trajectory (the "valley" between the top and bottom paths):
$$\delta_M^2 = \begin{cases} (\sqrt{3}/2) \left[\sin((\arctan\sqrt{26})/3 + \pi/6) + \sqrt{3}\sin((-\arctan\sqrt{26})/3 + \pi/3) + 4\sqrt{3} \right] \epsilon(1-\epsilon), & \text{top trajectory }; \\ (\sqrt{3}/2) \left[\sin((\arctan\sqrt{26})/3 + \pi/6) + (\sqrt{3}\sin((\arctan\sqrt{26})/3 + \pi/6) + (\sqrt{3}\sin((\arctan\sqrt{26})/3 + \pi/3) + 4\sqrt{3} \right] \epsilon(1-\epsilon), & \text{valley }; \\ (2-\sqrt{3}\sin((\arctan\sqrt{26})/3 + \pi/6)) \epsilon(1-\epsilon), & \text{bottom trajectory }. \end{cases}$$

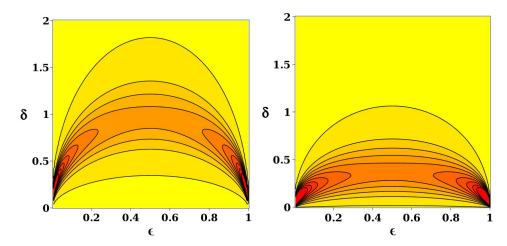


Figure 7: (Left) Contourplot of the density $\mathbb{P}_r^{f,(top)}(\epsilon,\delta)$ of the top path in grafted staircase polygons in the scaling limit. (Right) A contourplot of the density $\mathbb{P}_r^{f,(bottom)}(\epsilon,\delta)$ of the bottom path in grafted staircase polygons in the scaling limit. Lighter regions have low densities.

Evaluating the constants gives

$$\delta_{M} = \begin{cases} 1.8848 \dots \sqrt{\epsilon(1-\epsilon)}, & \text{top trajectory;} \\ 1.3741 \dots \sqrt{\epsilon(1-\epsilon)}, & \text{valley;} \\ 0.7476 \dots \sqrt{\epsilon(1-\epsilon)}, & \text{bottom trajectory.} \end{cases}$$
(14)

The mean path can also be determined by integrating $\delta \mathbb{P}_r^{f,(both)}(\epsilon, \delta)$. This gives the mean path $\overline{\delta} = (5/2\sqrt{\pi})\sqrt{\epsilon(1-\epsilon)}$ for the full model.

2.2. The probability density of the top path in the free phase

The probability that the top path passes through a given point (ϵ, δ) can be obtained by integrating $\mathbb{P}_r^{(2)}(\epsilon, \delta_1, \delta_2)$ (equation (4)) for $\delta_1 \in (0, \delta_2)$ and then normalising the result. Putting $\delta_2 = \delta$ gives

$$\mathbb{P}_{r}^{f,(top)}(\epsilon,\delta) = \frac{2}{3} \frac{\delta^{2}(4\delta^{4} - 12\delta^{2}\epsilon(1-\epsilon) + 15\epsilon^{2}(1-\epsilon)^{2})}{\sqrt{\pi}\sqrt{\epsilon^{7}(1-\epsilon)^{7}}} e^{-\delta^{2}/\epsilon(1-\epsilon)} \operatorname{erf}(\delta/\sqrt{\epsilon(1-\epsilon)}) - \frac{4}{3} \frac{\delta^{3}(2\delta^{2} - 15\epsilon(1-\epsilon))}{\pi\epsilon^{3}(1-\epsilon)^{3}} e^{-2\delta^{2}/\epsilon(1-\epsilon)}.$$
(15)

A plot of the density of the top path is shown in figure 7 (left panel). A probability measure ν_t with respect to plane measure can be defined as in equation (10) for calculating the probabilities that the top path passes through a subset in the plane, irrespective of the trajectory of the bottom path.

2.2.1. The most likely and mean paths of the top path in the free phase: Taking the derivative of $\log \mathbb{P}_r^{(top)}(\epsilon, \delta)$ (equation (15)), and determining its numerator, show that

the most likely trajectory of the top path is determined by the solution of δ in

$$4\sqrt{\pi}\,\delta\sqrt{\epsilon(1-\epsilon)}\left(2\,\delta^4 - 29\,\delta^2\epsilon(1-\epsilon) + 15\,\epsilon^2(1-\epsilon)^2\right)e^{-\delta^2/\epsilon(1-\epsilon)} + 2\,\pi\left(4\,\delta^6 - 24\,\delta^4\epsilon(1-\epsilon) + 39\,\delta^2\epsilon^2(1-\epsilon)^2 - 15\,\epsilon^3(1-\epsilon)^3\right)\operatorname{erf}(\delta/\sqrt{\epsilon(1-\epsilon)}) = 0. \quad (16)$$

Simplify this by putting $\delta^2 = K \epsilon (1 - \epsilon)$. This gives

$$4\sqrt{\pi} (2K^2 - 29K + 15) e^{-K} + 2\pi (4K^3 - 24K^2 + 39K - 15) \operatorname{erf}(\sqrt{K}) = 0$$
 (17)

which can be solved numerically. Choosing the correct solution gives K = 1.9082... This gives the most likely trajectory $\delta_M = 1.3814...\sqrt{\epsilon(1-\epsilon)}$. This is not the same trajectory of the top path in equation (14) (since integrating the bottom path changes the weight of the top path in the probability distribution).

The mean top path can be calculated from $\mathbb{P}_r^{f,(top)}(\epsilon,\delta)$ and is given by $\overline{\delta} = (5/\sqrt{2\pi})\sqrt{\epsilon(1-\epsilon)}$, which is larger by a factor of $\sqrt{2}$ than the mean trajectory of both paths.

2.3. The probability density of the bottom path in the free phase

The density of the bottom path is obtained by integrating equation (8) for $\delta_2 \in (\delta_1, \infty)$ and then normalising. This gives

$$\mathbb{P}_{r}^{f,(bottom)}(\epsilon,\delta) = \frac{2}{3} \frac{\delta^{2}(4\delta^{4} - 12\delta^{2}\epsilon(1-\epsilon) + 15\epsilon^{2}(1-\epsilon)^{2})}{\sqrt{\pi}\sqrt{\epsilon^{7}(1-\epsilon)^{7}}} e^{-\delta^{2}/\epsilon(1-\epsilon)} \operatorname{erfc}(\delta/\sqrt{\epsilon(1-\epsilon)}) + \frac{4}{3} \frac{\delta^{3}(2\delta^{2} - 15\epsilon(1-\epsilon))}{\pi\epsilon^{3}(1-\epsilon)^{3}} e^{-2\delta^{2}/\epsilon(1-\epsilon)}, \tag{18}$$

where $\operatorname{erfc}(x) = 1 - \operatorname{erf}(x)$ is the complementary error function. This density is plotted in the right panel of figure 7. Notice that

$$2 \mathbb{P}_r^{f,(both)}(\epsilon, \delta) = \mathbb{P}_r^{f,(top)}(\epsilon, \delta) + \mathbb{P}_r^{f,(bottom)}(\epsilon, \delta), \tag{19}$$

as expected.

A probability measure ν_b with respect to plane measure can be defined as in equation (10) for calculating the probabilities that the bottom path passes through a subset in the plane, irrespective of the trajectory of the top path.

2.3.1. The most likely and mean paths of the bottom path in the free phase: To determine the most likely trajectory, proceed as above by assuming that it is a curve $\delta = K\sqrt{\epsilon(1-\epsilon)}$. This again gives equation (17) which can be solved numerically and choosing the correct zero. This gives $K=0.7073\ldots$ and notice that $K^2=0.500232\ldots$, very close to 1/2. The most likely trajectory is $\delta_M=0.7073\ldots\sqrt{\epsilon(1-\epsilon)}$.

The mean trajectory of the bottom path can be calculated from $\mathbb{P}_r^{f,(bottom)}(\epsilon,\delta)$. This gives $\bar{\delta} = (5(\sqrt{2}-1)/\sqrt{2\pi})\sqrt{\epsilon(1-\epsilon)}$.

3. Probability densities in the adsorbed phase

The number $r_n(j, \ell)$ of pairs of osculating paths (see figure 3), starting in (0, 0) and (0, 2), each of length n (so that the width of the pair of paths is n), and ending in

vertices with heights $h_1 = (j - \ell)$ and $h_2 = (j + \ell + 2)$, is given by equation (5.173) in reference [14]:

$$r_n(j,\ell) = \sum_{m_1=0}^{n} \sum_{m_2=0}^{n+1} U_n(j+m_1+m_2,\ell+m_1+m_2) (a-1)^{m_1+m_2}$$
 (20)

where a is the generating variable of returns of the bottom path to the adsorbing hard wall. $U_n(j,\ell)$ is given by equation (1), and j and ℓ must have the same parity as n. In this paper the expressions are simplified by putting A = a - 1, so that the special or critical point is A = 1 (since $a_c = 2$ is the location of the critical points).

If $\ell=0$ then these are adsorbing directed paths from (0,0) and (0,2) to the vertices (n,j) and (n,j+2). By "capping" the left starting points with two steps, and the right end points with two steps, an adsorbing staircase polygon of length 2n+4, grafted at only at the origin, is obtained. The partition function of such adsorbing polygons is given by $r_n(j,0)$. Similarly, if $j=\ell=0$, then the partition function $r_n(0,0)$ is of a model of adsorbing staircase polygons grafted at both (0,0) and (n,0). These polygons have length 2n+4 and are grafted at both ends as shown in figure 5. For example, if n=4 then

$$r_n(0,0) = 14a^3 + 28a^2 + 28a + 14. (21)$$

Define

$$R_n(h_1, h_2) = r_n((h_1 + h_2)/2 - 1, (h_2 - h_1)/2 - 1),$$
(22)

the partition function of pairs of paths from (0,0) and (0,2) respectively, and to (n,h_1) and (n,h_2) respectively.

The asymptotic behaviour of $R_n(h_1, h_2)$ is determined in the Appendix, and it is given by equation (87) when a > 2 (recall that a = A+1). It may be put into the form

$$R_{2\lfloor \sigma n\rfloor}(2\lfloor \delta_1 \sqrt{n}\rfloor, 2\lfloor \delta_2 \sqrt{n}\rfloor) \simeq F(\sigma) \left(\delta_2 A^{-\delta_1 \sqrt{n}} e^{-\delta_2^2/\sigma} - \delta_1 A^{-\delta_2 \sqrt{n}} e^{-\delta_1^2/\sigma}\right), \quad (23)$$

where the approximations $\lfloor \sigma n \rfloor \simeq \sigma n$, $\lfloor \delta_1 \sqrt{n} \rfloor \simeq \delta_1 \sqrt{n}$ and $\lfloor \delta_2 \sqrt{n} \rfloor \simeq \delta_2 \sqrt{n}$ are made to obtain

$$F(\sigma) = \frac{2\log^2 A}{\sqrt{\pi \sigma^3 n^3}} 16^{\sigma n} e^{\sigma n(\log A)^2/4}.$$
 (24)

The probability that staircase polygons grafted at (0,0) and (2n,0) and of width 2n pass through points with coordinates $(2\lfloor \epsilon n \rfloor, 2\lfloor \delta_1 \sqrt{n} \rfloor)$ (the bottom path) and $(2|\epsilon n|, 2|\delta_2 \sqrt{n}|)$ (the top path) is asymptotically approximated by

$$N_o R_{2\lfloor \epsilon n \rfloor}(2\lfloor \delta_1 \sqrt{n} \rfloor, 2\lfloor \delta_2 \sqrt{n} \rfloor) \times R_{2\lfloor (1-\epsilon)n \rfloor}(2\lfloor \delta_1 \sqrt{n} \rfloor, 2\lfloor \delta_2 \sqrt{n} \rfloor), \tag{25}$$

where N_o is a normalising factor, independent of $(\epsilon, \delta_1, \delta_2)$. Using the approximation in equation (23) and then expanding the result gives

$$\begin{split} P_n^A(\epsilon,\delta_1,\delta_2) &\simeq N_o \, F(\epsilon) F(1-\epsilon) \, \left(A^{-2\,\delta_1\sqrt{n}} \, \delta_2^2 \, e^{-\delta_2^2/\epsilon(1-\epsilon)} - A^{-(\delta_1+\delta_2)\sqrt{n}} \, \delta_1 \delta_2 \, e^{-\delta_2^2/\epsilon-\delta_1^2/(1-\epsilon)} \right. \\ & \left. - A^{-(\delta_1+\delta_2)\sqrt{n}} \, \delta_1 \delta_2 \, e^{-\delta_1^2/\epsilon-\delta_2^2/(1-\epsilon)} + A^{-2\,\delta_2\sqrt{n}} \, \delta_1^2 \, e^{-\delta_1^2/\epsilon(1-\epsilon)} \right). \end{split} \tag{26}$$

3.1. The probability density of the top path

The probability that the top path passes through a vertex with coordinates $(\lfloor \epsilon n \rfloor, \lfloor \delta \sqrt{n} \rfloor)$ is obtained by integrating equation (26) for $\delta_1 \in (0, \delta_2)$, and then determining the normalising factor N_o . Simplifying $F(\epsilon) F(1-\epsilon)$ gives

$$a_0 = F(\epsilon)F(1-\epsilon) = \frac{4\log^4 A}{\pi n^3 \sqrt{\epsilon^3 (1-\epsilon)^3}} 16^n e^{(n\log^2 A)/4}.$$
 (27)

Next, the four terms in parenthesis in equation (26) must be integrated for $\delta_1 \in [0, \delta_2]$. Label these terms in order by $[a_1, a_2, a_3, a_4]$. Integrating and simplifying a_1 gives

$$\int_0^{\delta_2} a_1 \, d\delta_1 = \frac{\delta_2^2 (1 - A^{-2\delta_2\sqrt{n}})}{2\sqrt{n} \log A} \, e^{-\delta_2^2/\epsilon(1-\epsilon)}. \tag{28}$$

The integration of a_2 gives a more complicated result

$$\int_0^{\delta_2} a_2 \, d\delta_1 = \frac{\delta_2^2}{\sqrt{n} \log A} \, A^{-2\,\delta_2\sqrt{n}} \, e^{-\delta_2^2/\epsilon(1-\epsilon)} - \frac{\delta_2}{n \log^2 A} \, A^{-\delta_2\sqrt{n}} \, e^{-\delta_2^2/\epsilon}. \tag{29}$$

Integrating a_3 gives a similar result:

$$\int_0^{\delta_2} a_3 \, d\delta_1 = \frac{\delta_2^2}{\sqrt{n} \log A} \, A^{-2\,\delta_2\sqrt{n}} \, e^{-\delta_2^2/\epsilon(1-\epsilon)} - \frac{\delta_2}{n \log^2 A} \, A^{-\delta_2\sqrt{n}} \, e^{-\delta_2^2/(1-\epsilon)}. \tag{30}$$

Integrating the last term gives

$$\int_0^{\delta_2} a_4 d\delta_1 = \frac{\epsilon(1-\epsilon)}{4} A^{-2\delta_2\sqrt{n}} \left(\sqrt{\epsilon(1-\epsilon)} \operatorname{erf} \left(\delta_2 / \sqrt{\epsilon(1-\epsilon)} \right) - 2\delta_2 e^{-\delta_2^2/\epsilon(1-\epsilon)} \right). \tag{31}$$

These integrals must be combined with a_0 in equation (27) and integrated for $\delta_2 \in (0, \infty)$ to determine the normalising constant in equation (27). Executing the integrals, and simplifying gives

$$N_o^{-1} = \frac{\log^3 A}{2\sqrt{\pi n^7}} 16^n e^{n(\log^2 A)/4}.$$
 (32)

Combining these results, putting $\delta_2 = \delta$, and keeping only the leading terms, give the asymptotic probability for the top path passing through a vertex $(\lfloor \epsilon n \rfloor, \lfloor \delta \sqrt{n} \rfloor)$:

$$P_n^{A,(top)}(\epsilon,\delta) \simeq \frac{4 \,\delta^2}{\sqrt{\pi \epsilon^3 (1-\epsilon)^3}} e^{-\delta^2/\epsilon(1-\epsilon)} - \frac{8 \,\delta}{\sqrt{\pi n \epsilon^3 (1-\epsilon)^3} \log A} \left(e^{-\delta^2/\epsilon} + e^{-\delta^2/(1-\epsilon)} \right) . (33)$$

Taking $n \to \infty$ for A > 1 gives the exact probability of the top path passing through vertices (ϵ, δ) :

$$\mathbb{P}_r^{A,(top)}(\epsilon,\delta) = \frac{4\,\delta^2}{\sqrt{\pi\epsilon^3(1-\epsilon)^3}} \, e^{-\delta^2/\epsilon(1-\epsilon)}.\tag{34}$$

A contourplot of this probability density is shown in figure 8.

The probability density $\mathbb{P}_r^{A,(top)}(\epsilon,\delta)$ of the top path in the adsorbed phase can be used to calculate the probabilities that the top path passes through a given subset of \mathbb{R}^2 , independent of the trajectory of the bottom path.

As in equation (9), $R = (x_1, x_2) \times (y_1, y_2) \subset \mathbb{R}^2$ is an open rectangle in the plane with closure \overline{R} . Put $S = [0, 1] \times [0, \infty)$. Define $\mathbb{P}_r^{A, (top)}(\epsilon, \delta) = 0$ if $(\epsilon, \delta) \notin S$, and define the set function

$$\rho R = \rho \overline{R} = \int_{R \cap S} \mathbb{P}_r^{A,(top)}(\epsilon, \delta) \, d\delta \, d\epsilon. \tag{35}$$

Notice that ρ is a set function on the semialgebra of rectangles in \mathbb{R}^2 . Following the arguments towards equation (10), ρ induces an outer measure on subsets of \mathbb{R}^2 and is a probability measure on the σ -algebra of λ -measure sets E defined by

$$\rho E = \int_{E \cap S} \mathbb{P}_r^{A,(top)}(\epsilon, \delta) \, d\lambda. \tag{36}$$

It follows that $\rho S = \rho \mathbb{R}^2 = 1$, and that $\frac{d\rho}{d\lambda} = \mathbb{P}_r^{A,(top)}(\epsilon,\delta)$ is the Radon-Nikodym derivative of ρ with respect to λ . In this case ρE is the probability that the top path passes through the set E along its trajectory from (0,0) to (1,0), irrespective of the trajectory of the bottom path.

3.1.1. The most likely and mean trajectories of the top path in the adsorbed phase: Notice that $\mathbb{P}_r^{A,(top)}(\epsilon,\delta)$ is also the probability density of a single (desorbed) Dyck path in the scaling limit (see reference [15]). This is not unexpected, since the bottom path is adsorbed onto the hard wall, and the top path is screened from the wall, and does not interact with it. Figure 8 shows a low density region next to the hard wall. The most likely trajectory of the top path here is $\delta_M = \sqrt{\epsilon(1-\epsilon)}$ [15], while its mean trajectory is $\overline{\delta} = (2/\sqrt{\pi})\sqrt{\epsilon(1-\epsilon)}$.

3.2. The probability density of both paths

The asymptotic approximation to the probability density that either the top path, or the bottom path, passes through a given vertex is obtained by integrating equation (26) to δ_2 in $[0, \infty)$ (or equivalently, to δ_1 in $[0, \infty)$). As before, the normalising factor N_o must be calculated, and a_0 in equation (27) is independent of ϵ , δ_1 and of δ_2 .

Continue by integrating equation (26) for δ_2 from 0 to ∞ and then putting $\delta_1 = \delta$. This gives

$$\begin{split} N_o \, F(\epsilon) F(1-\epsilon) \, \left(\sqrt{\pi \, \epsilon(1-\epsilon)} \, A^{-2 \, \delta \sqrt{n}} / 4 + \delta^2 \, e^{-\delta^2/\epsilon(1-\epsilon)} / (2 \log(A) \sqrt{n}) \right. \\ \left. - A^{-\delta \sqrt{n}} (\delta/4) \, e^{-\delta^2/(1-\epsilon)} \, \left(2 \, \epsilon - \sqrt{\pi n \epsilon^3} \, \log A \, e^{(n\epsilon \log^2 A)/4} \operatorname{erfc} \left((\sqrt{\pi n \epsilon} \, \log A)/2 \right) \right) \right. \\ \left. - A^{-\delta \sqrt{n}} (\delta/4) \, e^{-\delta^2/\epsilon} \times \\ \left. \left(2 \, (1-\epsilon) - \sqrt{\pi n (1-\epsilon)^3} \, \log A \, e^{(n(1-\epsilon) \log^2 A)/4} \operatorname{erfc} \left((\sqrt{\pi n (1-\epsilon)} \, \log A)/2 \right) \right) \right). \end{split}$$

If \sqrt{n} is large, then the complementary error functions can be approximated using equation (78). This simplifies the above to

$$N_o F(\epsilon) F(1-\epsilon) \left(\sqrt{\pi \epsilon (1-\epsilon)} A^{-2\delta/\sqrt{n}} + 2\delta^2 e^{-\delta^2/\epsilon (1-\epsilon)} / (\sqrt{n} \log A) \right) / 4.$$
 (37)

Integrating $\delta \in (0, \infty)$ and simplifying gives

$$N_o^{-1} = \frac{\log^3 A}{\sqrt{\pi n^7}} 16^n e^{n \log^2 A/4}.$$
 (38)

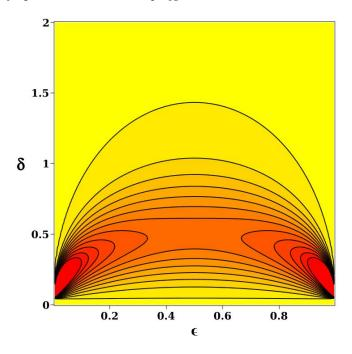


Figure 8: Contourplot of the density $\mathbb{P}_r^{A,(top)}(\epsilon,\delta)$ of the top path in a staircase polygon when the bottom path is adsorbed in the adsorbing wall (see equation 34). Lighter regions have lower densities. The plot shows low densities adjacent to the hard wall which increases with δ before it drops of farther from the wall. Since the lower path is adsorbed on the hard wall, this density of the top path is the same as the density for a single Dyck path determined in reference [15].

Substituting for N_o and simplifying gives the asymptotic approximation of the probability that either path passes through a point with coordinates $(\lfloor \epsilon n \rfloor, \lfloor \delta \sqrt{n} \rfloor)$:

$$P_n^{A,(both)}(\epsilon,\delta) \simeq \sqrt{n} A^{-2\delta\sqrt{n}} \log A + \frac{2\delta^2}{\sqrt{\pi\epsilon^3 (1-\epsilon)^3}} e^{-\delta^2/\epsilon(1-\epsilon)}.$$
 (39)

A plot of this probability is shown for A=1.5 and n=400 in figure 9. The normalisation of the two terms in equation (39) is such that

$$\int_0^\infty \sqrt{n} A^{-2\delta\sqrt{n}} \log A \, d\delta = 1/2, \quad \text{and} \quad \int_0^\infty \frac{2\delta^2}{\sqrt{\pi\epsilon^3 (1-\epsilon)^3}} \, e^{-\delta^2/\epsilon(1-\epsilon)} \, d\delta = 1/2. \tag{40}$$

Proceed by constructing a probability measure on plane measure sets in the limit as $n \to \infty$. The second term in equation (39) is, up to a factor of 1/2, the same as $\mathbb{P}_r^{A,(top)}(\epsilon,\delta)$ in equation (34). That is, it induces the measure $\rho/2$ on λ -measure sets in \mathbb{R}^2 as in equation (36).

Next, consider the first term on the right hand side in equation (39). Define the open rectangle $R = (x_1, x_2) \times (y_1, y_2)$ and its closure \overline{R} in \mathbb{R}^2 and let $S = [0, 1] \times [0, \infty)$.

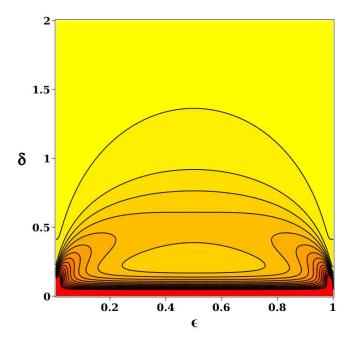


Figure 9: Contourplot of the density $P_n^{A,(both)}(\epsilon,\delta)$ (equation (39)) for a=2.5 and n=400. The bottom path is adsorbed, while the top path is screened from the adsorbing wall by the bottom path. Between these paths is a low density region.

Define the set function α_n on rectangles R by

$$\alpha_n R = \alpha_n \overline{R} = 2 \int_{R \cap S} \sqrt{n} \, A^{-2\delta\sqrt{n}} \log A \, d\delta \, d\epsilon. \tag{41}$$

Next, take the limit that $n \to \infty$ to define the set function $\alpha R = \lim_{n \to \infty} \alpha_n R$. For example, $\alpha S = \lim_{n \to \infty} \alpha_n S = 1$ by direct integration.

Proceed by defining the infinite half-open rectangle $R_{\delta} = (\epsilon_1, \epsilon_2) \times [\delta, \infty)$ where $\delta > 0$ and $0 < \epsilon_1 < \epsilon_2 < 1$. By excuting the integral,

$$\alpha R_{\delta} = \lim_{n \to \infty} \alpha_n R_{\delta} = \lim_{n \to \infty} A^{-2\delta\sqrt{n}} \left(\epsilon_2 - \epsilon_1\right) = 0, \tag{42}$$

since A > 1 and $\delta > 0$.

Moreover, if $R_0 = (\epsilon_1, \epsilon_2) \times [0, \infty)$ then integrating directly, $\alpha R_0 = (\epsilon_2 - \epsilon_1)$.

Next, consider the rectangles $T_{\delta} = (\epsilon_1, \epsilon_2) \times [0, \delta)$ where $\delta > 0$ and $0 < \epsilon_1 < \epsilon_2 < 1$. Then $T_{\delta} = R_0 \setminus R_{\delta}$ and it follows that if $\delta > 0$, then

$$\alpha T_{\delta} = \alpha (R_0 \setminus R_{\delta}) = \alpha R_0 - \alpha R_{\delta} = (\epsilon_2 - \epsilon_1). \tag{43}$$

For all other rectangles R in \mathbb{R}^2 , define

$$\alpha R = \alpha(R \cap S). \tag{44}$$

Then α is a set-function on the semi-algebra of rectangles, and it extends to an outer measure on subsets of \mathbb{R}^2 and to a measure on the σ -algebra of λ -measure sets in \mathbb{R}^2 .

Notice that $\alpha R = 0$ on all rectangles except on those where the intersection $R \cap [0,1]$ is an interval [a,b] (or the open or half-open interval), in which case $\alpha R = (b-a)$. In addition, $\alpha \mathbb{R}^2 = 1$ so that it is a probability measure and it induces a probability density $\mathbb{P}_r^{(\alpha)}(\epsilon,\delta)$ such that

$$\alpha E = \int_{E} \mathbb{P}_{r}^{A,(\alpha)}(\epsilon, \delta) \, d\lambda = \mu(E \cap [0, 1]) \tag{45}$$

where $\mathbb{P}_r^{A,(\alpha)}(\epsilon,\delta)=0$ if $(\epsilon,\delta)\in\mathbb{R}^2\setminus[0,1]$, and where μ is Lebesgue measure. This shows that $\mathbb{P}_r^{A,(\alpha)}(\epsilon,\delta)$ has support only on the line segment [0,1] in \mathbb{R}^2 and is zero everywhere else. That is $\alpha\mathbb{R}^2=\mu[0,1]=1$.

Using the probability measure α , the probability that either the bottom or top paths pass through a λ -measure set E in the $n \to \infty$ limit can be calculated from equation (39):

$$\lim_{n \to \infty} \int_E P_n^{A,(both)}(\epsilon, \delta) d\lambda = \lim_{n \to \infty} \int_E \sqrt{n} A^{-2\delta\sqrt{n}} \log A d\lambda + \frac{1}{2}\rho E = \frac{1}{2}\alpha E + \frac{1}{2}\rho E.$$
 (46)

This defines a probability measure $\kappa = (\alpha + \rho)/2$ on λ -measure sets such that κE is the probability that either the bottom, or the top path, or both, pass through E. Notice that α and ρ are mutually singular measures since there is a decomposition $\mathbb{R}^2 = A \cup B$ with $A \cap B = \emptyset$ such that $\alpha A = \rho B = 1$ and $\alpha B = \rho A = 0$ (for example, choose A = [0, 1],

3.2.1. Most likely trajectories in the adsorbed phase: The most likely trajectories of both paths can be calculated using equation (39) in the limit $n \to \infty$ and the measures α and ρ in equation (46). This gives the most likely trajectory of the bottom path $\delta_M = 0$ and of the top path is $\delta_M = \sqrt{\epsilon(1-\epsilon)}$, for $\epsilon \in [0,1]$.

In the case that n is finite, the most likely trajectories of the paths can be approximated as follows. The derivative of equation (39) simplifies to

$$\frac{d}{d\delta} P_n^{A,(both)}(\epsilon,\delta) \simeq \frac{4 \,\delta(\epsilon(1-\epsilon) - \delta^2)}{\sqrt{\pi \epsilon^5 (1-\epsilon)^5}} \,e^{-\delta^2/\epsilon(1-\epsilon)} - 2 \,n \,(\log A)^2 A^{-2 \,\delta \sqrt{n}}. \tag{47}$$

Putting the right hand side equal to zero, solve for δ . This can only be done approximately. Proceed by writing this in the form

$$\left(\frac{4\delta(\epsilon(1-\epsilon)-\delta^2)}{\sqrt{\pi\epsilon^5(1-\epsilon)^5}}e^{-\delta^2/\epsilon(1-\epsilon)}\right)^{1/n} = (2n(\log A)^2A^{-2\delta\sqrt{n}})^{1/n}.$$
(48)

Expand the right hand side asymptotically to first order in n, so that

$$\frac{4\delta(\epsilon(1-\epsilon)-\delta^2)}{\sqrt{\pi\epsilon^5(1-\epsilon)^5}} e^{-\delta^2/\epsilon(1-\epsilon)} \approx \left(1-2\delta(\log A)/\sqrt{n}+O(1/n)\right)^n. \tag{49}$$

Taking $n \to \infty$ on the right hand side gives (for $\delta > 0$),

$$\lim_{n \to \infty} (1 - 2\delta(\log A) / \sqrt{n} + O(1/n))^n = 0$$
 (50)

and in this case the solution of equation (49) is $\delta_M = \sqrt{\epsilon(1-\epsilon)}$, as expected.

If n is finite, proceed by assuming that to leading order, the solution to equation (49) is $\delta^2 = K \epsilon (1-\epsilon)$, where K may be a function of ϵ . Substitute and simplify to obtain the approximation

$$\frac{4\sqrt{K}(K-1)e^{-K}}{\sqrt{\pi}\epsilon(1-\epsilon)} \approx \left(1 - 2\sqrt{K\epsilon(1-\epsilon)}(\log A)/\sqrt{n} + O(1/n)\right)^{n}.$$
 (51)

Examination of the above shows that there are potential solutions for small values of K, and also for $K \approx 1$. This corresponds to the approximate most likely trajectories of the top path in figure 9 (the larger value of K), and for the "valley" between the top path, and the finite size adsorbed bottom path in figure 9.

In order to estimate the most likely trajectory of the path, put $K = 1 + \eta^2$ in equation (51). Expand the left hand side to $O(\eta^2)$ and the factor on the right hand side to O(1) to obtain

$$\frac{4\eta^2}{e\sqrt{\pi}\,\epsilon(1-\epsilon)} \approx \left(1 - 2\sqrt{\epsilon(1-\epsilon)}\,(\log A)/\sqrt{n}\right)^n \tag{52}$$

Solving for η^2 gives

$$\eta^2 \approx \frac{e}{4} \sqrt{\pi} \, \epsilon (1 - \epsilon) \, \left(1 - 2\sqrt{\epsilon(1 - \epsilon)} (\log A) / \sqrt{n} \right)^n \approx \frac{1}{4} \sqrt{\pi} \epsilon (1 - \epsilon) \, e^{1 - 2\sqrt{n \, \epsilon(1 - \epsilon)} \log A}. \tag{53}$$

Since $\delta^2 = K \epsilon(1-\epsilon)$, and $K = 1+\eta^2$, this gives the approximate most likely trajectory for finite n:

$$\delta_M = \sqrt{1 + \frac{1}{4}\sqrt{\pi}\epsilon(1-\epsilon)} e^{1-2\sqrt{n\epsilon(1-\epsilon)}\log A} \sqrt{\epsilon(1-\epsilon)}.$$
 (54)

Taking $n \to \infty$ gives $\delta_M = \sqrt{\epsilon(1-\epsilon)}$, as expected. If n = 400, A = 1.5 and $\epsilon = 1/2$, then this simplifies to $\delta_M \approx 0.5$, consistent with the top path in figure 9. For finite values of n the most likely top trajectory is futher away from the hard wall, consistent with it experiencing a repulsive force from the bottom path.

The "valley" in figure 9 is similarly determined, but instead putting $K = 0 + \eta^2$. Expanding the left hand side of equation (51) to $O(\eta)$, and the right hand side to $O(\eta)$, give

$$\frac{4\eta}{\sqrt{\pi}\,\epsilon(1-\epsilon)} \approx 1 - 2\sqrt{n\epsilon(1-\epsilon)}(\log A)\eta. \tag{55}$$

Solving for η gives

$$\eta = \frac{\sqrt{\pi} \,\epsilon(1 - \epsilon)}{4 + 2\sqrt{\pi} \,n} \sqrt{\epsilon^3 (1 - \epsilon)^3 \log A}.$$
 (56)

Thus, $K = \eta^2$ and the estimate of least likely trajectory along the "valley" is

$$\delta_V = \frac{\sqrt{\pi}\sqrt{\epsilon^3(1-\epsilon)^3}}{4 + 2\sqrt{\pi}\,n\sqrt{\epsilon^3(1-\epsilon)^3}\log A}.$$
 (57)

This underestimates the location of the most likely trajectory of the valley in figure 9, showing that the assumption that η is small in determining K is in all likelihood not applicable. However, as $n \to \infty$, or as $\log A \to \infty$, this converges to $\delta_V = 0$, consistent with the properties of the measures α and ρ .

The mean path is obtained by integrating $\delta P_n^{A,(both)}(\epsilon,\delta)$ (equation (39)). This gives

$$\int_0^\infty P_n^{A,(both)}(\epsilon,\delta) \, d\delta = \int_0^\infty \delta \sqrt{n} A^{-2\,\delta\sqrt{n}}(\log A) \, d\delta + \int_0^\infty \frac{2\,\delta^3}{\sqrt{\pi\epsilon^3(1-\epsilon)^3}} \, e^{-\delta^2/\epsilon(1-\epsilon)} \, d\delta.$$

This gives the estimated mean path for finite n:

$$\overline{\delta} = \frac{1}{4\sqrt{n}\log A} + \frac{\sqrt{\epsilon(1-\epsilon)}}{\sqrt{\pi}}.$$
 (58)

Taking $n \to \infty$ gives the mean path $\overline{\delta} = (1/\sqrt{\pi})\sqrt{\epsilon(1-\epsilon)}$.

3.3. The probability density of the bottom path

The starting point is again equation (26) with a_0 defined as in equation (27). The probability will be obtained by integrating the terms in the parenthesis in equation (26) for $\delta_2 \in [\delta_1, \infty)$ and then normalising the result. As before, only leading order terms are kept.

Proceed by denoting the four terms in parenthesis in equation (26) by $[a_1, a_2, a_3, a_4]$. Integrating a_1 gives

$$\int_{\delta_1}^{\infty} a_1 d\delta_2 = \frac{1}{2} \, \delta_1 \, \epsilon(1 - \epsilon) \, A^{-2 \, \delta_1 \sqrt{n}} \, e^{-\delta_1^2 / \epsilon(1 - \epsilon)}$$

$$+ \frac{\sqrt{\pi}}{4} \, \sqrt{\epsilon^3 (1 - \epsilon)^3} \, A^{-2 \, \delta_1 \sqrt{n}} \operatorname{erfc} \left(\delta_1 / \sqrt{\epsilon(1 - \epsilon)} \right). \tag{59}$$

The remaining three integrals give

$$\int_{\delta_{1}}^{\infty} a_{2} d\delta_{2} = -\delta_{1} \left(\frac{\epsilon}{2} + \frac{\delta_{1}}{\sqrt{n} \log A} \right) A^{-2 \delta_{1} \sqrt{n}} e^{-\delta_{1}^{2}/\epsilon(1-\epsilon)}$$

$$\int_{\delta_{1}}^{\infty} a_{3} d\delta_{2} = -\delta_{1} \left(\frac{1-\epsilon}{2} + \frac{\delta_{1}}{\sqrt{n} \log A} \right) A^{-2 \delta_{1} \sqrt{n}} e^{-\delta_{1}^{2}/\epsilon(1-\epsilon)}$$

$$\int_{\delta_{1}}^{\infty} a_{4} d\delta_{2} = \frac{1}{2\sqrt{n} \log A} \delta_{1}^{2} A^{-2 \delta_{1} \sqrt{n}} e^{-\delta_{1}^{2}/\epsilon(1-\epsilon)}.$$
(60)

Adding these contributions gives the asymptotic result

$$P_n^{A,(bottom)}(\epsilon,\delta) \simeq N_o \frac{\sqrt{\pi\epsilon^3(1-\epsilon)^3}}{4} A^{-2\delta\sqrt{n}} \operatorname{erfc}(\delta/\sqrt{\epsilon(1-\epsilon)})$$
 (61)

where N_o is a normalising factor. Integrating to determine N_o gives

$$N_o^{-1} \simeq \frac{\sqrt{\pi \epsilon^3 (1 - \epsilon)^3}}{8\sqrt{n} \log A} - \frac{\epsilon (1 - \epsilon)}{8 n \log^2 A}.$$
 (62)

Ignoring the second term and substituting gives the leading term of the probability $P_n^{A,(bottom)}(\epsilon,\delta)$ that the bottom path passes through the vertex $(\lfloor \epsilon n \rfloor, \lfloor \delta \sqrt{n} \rfloor)$:

$$P_n^{A,(bottom)}(\epsilon, \delta) \simeq 2\sqrt{n}(\log A)A^{-2\delta\sqrt{n}}\operatorname{erfc}(\delta/\sqrt{\epsilon(1-\epsilon)}).$$
 (63)

This approximation of $P_n^{A,(bottom)}(\epsilon, \delta)$ is plotted in figure 10 for A = 1.1 and n = 100 (left panel) and for n = 10000 (right panel).

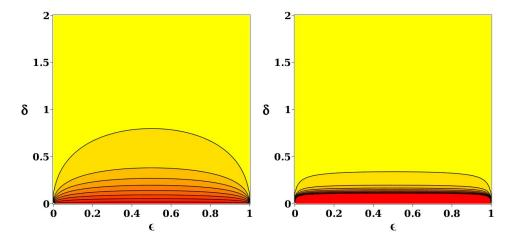


Figure 10: Contourplot of the density $P_n^{A,(bottom)}(\epsilon,\delta)$ (equation (63)) for a=2.1 and n=100 (left panel) and n=10000 (right panel). The bottom path is adsorbed (in the limit as $n\to\infty$). These plots give the density of the probability that the bottom path passes through points in the square lattice. Darker shades correspond to higher densities.

A probability measure β can now be determined similarly to α in equation (45). Define $S = [0,1] \times [0,\infty)$ in the $\epsilon\delta$ -plane. Introduce plane measure λ and define the β -measure of a λ -measure set E by

$$\beta E = \lim_{n \to \infty} \int_{E \cap S} P_n^{A,(bottom)}(\epsilon, \delta) \, d\delta \, d\epsilon = \int_E \mathbb{P}_r^{A,(bottom)}(\epsilon, \delta) \, d\lambda. \tag{64}$$

Then β is a probability measure on \mathbb{R}^2 with density $\mathbb{P}_r^{A,(bottom)}(\epsilon,\delta)$. Similar to equation (46), for a λ -measure set E,

$$\beta E = \lim_{n \to \infty} \int_{E \cap S} 2\sqrt{n} (\log A) A^{-2\delta\sqrt{n}} \operatorname{erfc}(\delta/\sqrt{\epsilon(1-\epsilon)}) \, d\delta \, d\epsilon \tag{65}$$

and it follows that $\mathbb{P}_r^{A,(bottom)}(\epsilon,\delta)=0$ for $(\epsilon,\delta)\in\mathbb{R}^2\setminus[0,1]$. In addition, notice that

$$\lim_{n \to \infty} \int_0^\infty 2\sqrt{n} (\log A) A^{-2\delta\sqrt{n}} \operatorname{erfc}(\delta/\epsilon(1-\epsilon)) d\delta = 1, \quad \forall \epsilon \in (0,1).$$
 (66)

That is, the measure β is concentrated on the line segment [0,1] and zero everywhere else. This shows that $\beta=\alpha$ since $\mathbb{P}^{A,(\alpha)}_r=\mathbb{P}^{A,(bottom)}_r$. The most likely and mean trajectory of the bottom path is $\delta_M=0$ and $\overline{\delta}=0$ in the limit as $n\to\infty$.

4. Probabilty densities at the critical or special point $a_c = 2$

The asymptotic approximation of $R_n(h_1, h_2)$ in the case that A = 1, $h_1 = 2\lfloor \delta_1 \sqrt{n} \rfloor$ and $h_2 = 2 \lfloor \delta_2 \sqrt{n} \rfloor$ is given by equation (90) in the Appendix. The probability that the

paths pass through the points $(2\lfloor \epsilon n \rfloor, 2\lfloor \delta_1 \sqrt{n} \rfloor)$ and $(2\lfloor \epsilon n \rfloor, 2\lfloor \delta_2 \sqrt{n} \rfloor)$ is asymptotically approximated by

$$P_n^{2,(sp)}(\epsilon, \delta_1, \delta_2) \simeq N_o R_{2\lfloor \epsilon n \rfloor}(2\lfloor \delta_1 \sqrt{n} \rfloor, 2\lfloor \delta_2 \sqrt{n} \rfloor) \times R_{2\lfloor (1-\epsilon)n \rfloor}(2\lfloor \delta_1 \sqrt{n} \rfloor, 2\lfloor \delta_2 \sqrt{n} \rfloor)$$
(67)

where N_o is a normalising factor. Expanding this gives to leading order

$$P_n^{2,(sp)}(\epsilon, \delta_1, \delta_2) \simeq N_o \frac{\left(\delta_2^2 - \delta_1^2\right)^2}{\pi^2 n^5 \epsilon^3 (1 - \epsilon)^3} 16^{n+1} e^{-(\delta_1^2 + \delta_2^2)/\epsilon(1 - \epsilon)}, \tag{68}$$

where N_o is the normalising factor which remains to be determined.

4.1. The probability that either path pass through a given point:

Integrating equation (68) for $\delta_2 \in [0, \infty)$ and putting $\delta_1 = \delta$ gives the asymptotic probability that either the top, or the bottom path, passes through the point $(\lfloor \epsilon n \rfloor, \lfloor \delta \sqrt{n} \rfloor)$:

$$P_n^{2,(both)}(\epsilon,\delta) \simeq 2 \, N_o \frac{4 \, \delta^4 - 4 \, \epsilon (1-\epsilon)\delta^2 + 3 \, \epsilon^2 (1-\epsilon)^2}{n^5 \sqrt{\pi^3 \epsilon^5 (1-\epsilon)^5}} \, 16^n \, e^{-\delta^2/\epsilon (1-\epsilon)}. \tag{69}$$

Normalising gives $N_o = \pi n^5 \, 16^{-n-1/2}$ and the probability density

$$\mathbb{P}_r^{2,(both)}(\epsilon,\delta) = \frac{4\delta^4 - 4\epsilon(1-\epsilon)\delta^2 + 3\epsilon^2(1-\epsilon)^2}{2\sqrt{\pi\epsilon^5(1-\epsilon)^5}} e^{-\delta^2/\epsilon(1-\epsilon)}.$$
 (70)

A probability measure can be defined with density similar to the way it was defined in the free case in section (1.2).

The most likely trajectories and mean trajectories of the paths, with the locally least likely trajectory (the valley in figure 9) can be determined as before.

Consider first the case $\mathbb{P}_2^{2,(both)}(\epsilon,\delta)$ in equation (73) and figure 11. Taking the derivative and solving for δ gives three solutions, namely

$$\delta_{M} = \begin{cases} \sqrt{\frac{3+\sqrt{2}}{2}} \sqrt{\epsilon(1-\epsilon)}, & \text{top trajectory;} \\ \sqrt{\frac{3-\sqrt{2}}{2}} \sqrt{\epsilon(1-\epsilon)}, & \text{valley;} \\ 0, & \text{bottom trajectory.} \end{cases}$$
(71)

The mean path can also be determined and it is $\bar{\delta} = (7/4\sqrt{\pi})\sqrt{\epsilon(1-\epsilon)}$.

4.2. The probability density that the top path passes through a given point

The probability density that the top path passes through a given point is obtained by integrating equation (68) for $\delta_1 \in (0, \delta_2)$ and then normalising the result. Putting $\delta_1 = \delta$ gives

$$P_n^{2,(top)}(\epsilon,\delta) \simeq 2 N_o \left(\frac{4 \delta^4 - 4 \epsilon (1-\epsilon) \delta^2 + 3 \epsilon^2 (1-\epsilon)^2}{n^5 \sqrt{\pi^3 \epsilon (1-\epsilon)}} 16^n e^{-\delta^2/\epsilon (1-\epsilon)} \operatorname{erf}(\delta/\sqrt{\epsilon (1-\epsilon)} + \frac{2 \delta (2 \delta^2 - 3 \epsilon (1-\epsilon))}{\pi^2 n^5 \epsilon^2 (1-\epsilon)^2} 16^n e^{-2 \delta^2/\epsilon (1-\epsilon)} \right). \tag{72}$$

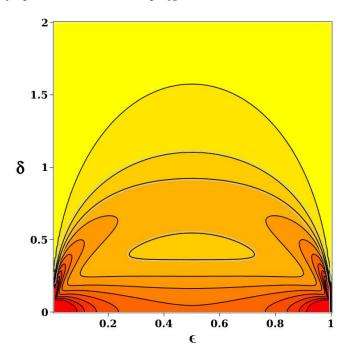


Figure 11: Contourplot of the density $\mathbb{P}_r^{2,(both)}(\epsilon,\delta)$ (equation (73)) at the critical adsorption point $a_c=2$. The bottom path is adsorbed, while the top path is screened from the adsorbing wall by the bottom path. Between these paths is a low density region.

The normalising factor is $N_o^{-1} = \pi n^5 16^{n-1/4}$. This gives the probability density

$$\mathbb{P}_{r}^{2,(top)}(\epsilon,\delta) = \frac{4\delta^{4} - 4\epsilon(1-\epsilon)\delta^{2} + 3\epsilon^{2}(1-\epsilon)^{2}}{\sqrt{\pi\epsilon^{5}(1-\epsilon)^{5}}} e^{-\delta^{2}/\epsilon(1-\epsilon)} \operatorname{erf}(\delta/\sqrt{\epsilon(1-\epsilon)}) + \frac{2\delta(2\delta^{2} - 3\epsilon(1-\epsilon))}{\pi\epsilon^{2}(1-\epsilon)^{2}} e^{-2\delta^{2}/\epsilon(1-\epsilon)}.$$
(73)

This density is plotted in figure (12)(left).

The most likely trajectory of the top path can be obtained from the density in equation (73). Taking the derivative of $\mathbb{P}_r^{2,(top)}(\epsilon,\delta)$ and simplifying gives

$$0 = \frac{4 \delta^2 (7 \epsilon (1 - \epsilon) - 2 \delta^2)}{\pi \epsilon^3 (1 - \epsilon)^3} e^{-2 \delta^2 / \epsilon (1 - \epsilon)} + \frac{2 \delta (4 \delta^2 (3 \epsilon (1 - \epsilon) - \delta^2) - 7 \epsilon^2 (1 - \epsilon)^2)}{\sqrt{\pi \epsilon^7 (1 - \epsilon)^7}} e^{-\delta^2 / \epsilon (1 - \epsilon)} \operatorname{erf}(\delta / \sqrt{\epsilon (1 - \epsilon)}).$$

The zeros of the coefficients above do not coincide, but a numerical solution can be obtained. Assume that the trajectory is of the form $\delta^2 = K \epsilon (1-\epsilon)$ and substitute. This gives the following equation for K, independent of ϵ :

$$2\sqrt{\pi K}(4K^2 - 12K + 7)\operatorname{erf}(\sqrt{K}) + 4K(2K - 7)e^{-K} = 0.$$
 (74)

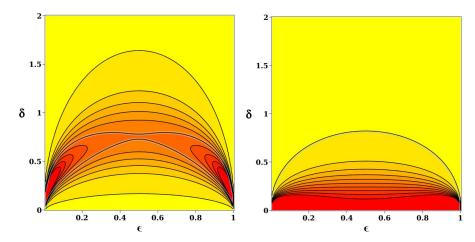


Figure 12: Contourplots of the densities $\mathbb{P}_r^{2,(top)}(\epsilon,\delta)$ (left panel, equation (73)) and $\mathbb{P}_r^{2,(bottom)}(\epsilon,\delta)$ (right panel, equation (75)) at the critical adsorption point $a_c=2$. The bottom path is adsorbed the critical point (in the limit as $n\to\infty$). Darker shades correspond to higher densities.

There are two solutions: K=0 and K=2.2808... This gives the most likely trajectory of the top path $\delta=1.5102...\sqrt{\epsilon(1-\epsilon)}$. The mean trajectory can be determined as well: $\bar{\delta}=(2\sqrt{2}/\sqrt{\pi})\sqrt{\epsilon(1-\epsilon)}$.

4.3. The probability density that the bottom path passes through a given point

The probability density of the bottom path is similarly obtained, and is given by

$$\mathbb{P}_{r}^{2,(bottom)}(\epsilon,\delta) = \frac{4\delta^{4} - 4\epsilon(1-\epsilon)\delta^{2} + 3\epsilon^{2}(1-\epsilon)^{2}}{\sqrt{\pi\epsilon^{5}(1-\epsilon)^{5}}} e^{-\delta^{2}/\epsilon(1-\epsilon)} \operatorname{erfc}(\delta/\sqrt{\epsilon(1-\epsilon)}) - \frac{2\delta(2\delta^{2} - 3\epsilon(1-\epsilon))}{\pi\epsilon^{2}(1-\epsilon)^{2}} e^{-2\delta^{2}/\epsilon(1-\epsilon)}.$$
(75)

A contourplot is displayed in figure 12(right). As before, probability measures can be defined with densities in equation (73) and (75).

The most likely bottom trajectory in equation (75) is similarly determined, leading to the equation

$$0 = -\frac{4 \delta^2 (7 \epsilon (1-\epsilon) - 2 \delta^2)}{\pi \epsilon^3 (1-\epsilon)^3} e^{-2 \delta^2 / \epsilon (1-\epsilon)} + \frac{2 \delta (4 \delta^2 (3 \epsilon (1-\epsilon) - \delta^2) - 7 \epsilon^2 (1-\epsilon)^2)}{\sqrt{\pi \epsilon^7 (1-\epsilon)^7}} e^{-\delta^2 / \epsilon (1-\epsilon)} \operatorname{erfc}(\delta / \sqrt{\epsilon (1-\epsilon)}).$$

Substituting $\delta_M^2 = K \epsilon (1 - \epsilon)$ and simplify. This gives

$$2\sqrt{\pi K}(4K^2 - 12K + 7)\operatorname{erfc}(\sqrt{K}) - 4K(2K - 7)e^{-K} = 0.$$
 (76)

The only non-negative solution on the real line is K=0, so that the most likely trajectory is $\delta=0$.

The mean bottom path is $\overline{\delta} = ((7 - 4\sqrt{2})/(2\sqrt{\pi})) \sqrt{\epsilon(1-\epsilon)}$.

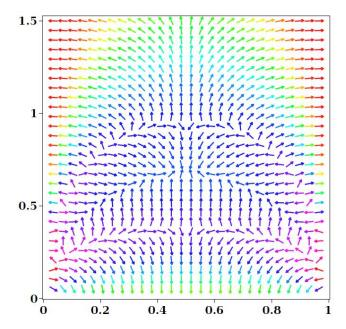


Figure 13: A gradient plot of the probability density in the free phase (see figure 6). The arrows are all of fixed length and point in the direction of the net force on a test particle. The bottom axis is the ϵ -coordinate and the vertical axis is δ -coordinate, so that the hard wall is the bottom horizontal axis. There are attractive forces towards to wall in its vicinity. There are also net attractive forces towards the local minimum in the density near the centre of the figure. Towards the top of the figure the gradient shows a repulsive force away from the hard wall.

5. Discussion

Forces due to density gradients can be calculated by taking the gradient of the probability densities. For example, the gradient of the probability density in the free case for both paths in equation (8) is shown in the gradient plot in figure 13. This is a rescaled force-field experienced by a test particle placed at a vertex (ϵ, δ) in the scaling limit. The directions of the arrows indicate the direction of the force, and the lengths of the arrows are fixed.

Plotting the force strength in the vertical direction for $\epsilon=1/2$ gives the left panel in figure 14. There are four points where the forces disappear. Numbering from origin, the zeroth and second zeros are stable minima in the density, where a test particle will experience restorative forces towards a stable (local) minimum.

Calculating the forces at the special point gives the right panel in figure 14. In constrast with the free case, the forces are positive (repulsive) next to the hard wall. There remains an interval where the forces are attractive, and this is located between the two paths.

In this paper the most likely and mean trajectories of paths were calculated from the exact probability distributions. Summaries are given in tables 1 (most likely

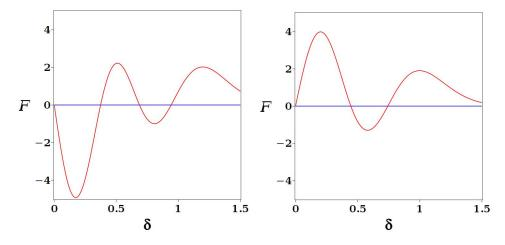


Figure 14: (Left) The vertical component F of the force in the gradient plot in figure 13 calculated from the probability density $\mathbb{P}_r^{f,(both)}(\epsilon,\delta)$ for both paths in the free phase. Negative values of the force are towards the hard wall, and positive forces point away from it. (Right) The forces at the special point. Here, a test particle experiences a repulsive force when placed next to the hard wall.

trajectories) and 2 (mean trajectories), for all the cases and phases considered. In table 1 the columns corresponds to the most likely trajectories of the top and bottom paths, as well as the "valley" separating them. Exact values of K are shown where possible, but the numerical results in the first row were calculated from the exact trajectories displayed in equation (13).

In table 2 the exact mean trajectories are shown for both paths, and the top and bottom paths, and in the various phases.

Model	K (Top path)	K ("Valley")	K (Bottom path)
Free	1.8848	1.3741	0.7476
Adsorbed	1	0	0
Special point	$\sqrt{\frac{3+\sqrt{2}}{2}}$	$\sqrt{\frac{3-\sqrt{2}}{2}}$	0

Table 1: Most likely trajectories $\delta_M = K\sqrt{\epsilon(-\epsilon)}$

The model in this paper shows that the density of grafted staircase polygons has low density regions. This suggests that the monomer distribution of a grafted polymer network in two dimensions is uneven with low density regions between polymers and the hard wall, and also between polymers. At sufficiently low temperatures, a test particle will likely localize in such a low density region until it diffuses away from the network due to thermal vibrations, or until the network degrades and releases it. The

Model	K (Both paths)	K (Top path)	K (Bottom path)
Free	$\frac{5}{2\sqrt{\pi}}$	$\frac{5}{\sqrt{2\pi}}$	$\frac{5(\sqrt{2}-1)}{\sqrt{2\pi}}$
Adsorbed	$\frac{1}{\sqrt{\pi}}$	$\frac{2}{\sqrt{\pi}}$	0
Special point	$\frac{7}{4\sqrt{\pi}}$	$\frac{2\sqrt{2}}{\sqrt{\pi}}$	$\frac{7-4\sqrt{2}}{2\sqrt{2}}$

Table 2: Mean trajectories $\overline{\delta} = K\sqrt{\epsilon(-\epsilon)}$

results here show that there is little scope for an adsorbed polymer chain to contain a test particle, as its density decreases with distance from the wall, as already seen in the model in reference [15]. However, a second (desorbed) polymer, grafted to the wall or to the first, may cause the formation of lower density regions, as seen in figures 9 and 11. More realistic simulations using Monte Carlo simulations of self-avoiding walks or chains may give more insight into the densities of grafted polymers, and the mechanism for capturing and stabilising absorbed particles in a polymer network.

Appendix:

To determine an asymptotic approximation to r(j, l) asymptotic formulae for n! and for the error function are needed:

$$n! \simeq n^n e^{-n} \sqrt{(2n+1/3)\pi} (1 + O(1/n^2)),$$
 (77)

$$\operatorname{erf}(x) \simeq 1 - (1/(\sqrt{\pi} x)) e^{-x^2} (1 + O(1/x^2)).$$
 (78)

Proceed by substituting $n \to 2n$, $j \to 2j$ and $\ell \to 2\ell$ in equation (20). Replacing $m_1 = k - m_2$, the sum over m_2 can be executed. This gives

$$r_{2n}(2j, 2\ell) = \sum_{k=0}^{n} (F_n(j, k, \ell) - G_n(j, k, \ell)) A^k$$
(79)

where A = a - 1, and

$$F_n(j,k,\ell) = \frac{(2j+k+2)(n+1+2\ell(\ell+k+2)-2j(j+k+2))}{2(n+1)^2(2n+1)} \binom{2n+2}{n+1+j-\ell} \binom{2n+2}{n+3+j+k+\ell}$$

$$G_n(j,k,\ell) = \frac{(2j+k+2)(n-1+2\ell(\ell-k)-2j(j+k+2)-2k)}{2(n+1)^2(2n+1)} \binom{2n+2}{n+2+j+\ell} \binom{2n+2}{n+2+j+\ell}$$

The length 2n is the *half-length* or width of the pair of walks. The partition function for half-length 2n and ending in even heights h_1 and h_2 , with $h_1 < h_2$, is

$$Z_{2n}(h_1, h_2) = r_{2n}((h_1 + h_2)/4 - 1/2, (h_2 - h_1)/4 - 1/2).$$
 (80)

For example, this shows that $Z_4(2,4) = 3 + 3a$.

Since the paths are ballistic in the horizontal direction, and are random walks in the vertical direction, the natural length scales in this model is O(n) horizontally, and

 $O(\sqrt{n})$ vertically. Thus, substitute $n \to \lfloor \sigma n \rfloor$, $k = \lfloor \eta n \rfloor$, $2(j-k) = h_1 = 2 \lfloor \delta_1 \sqrt{n} \rfloor$ and $2(j+k+1) = h_2 = 2 \lfloor \delta_2 \sqrt{n} \rfloor$.

Continue by first calculating an asymptotic approximation to $F_n(j, k, \ell)$. Convert the binomial coefficients to factorials and use the Stirling approximation in equation (77). Simplifying gives

$$F_n \simeq \frac{36 a_2 a_3 a_4 a_7 a_{20} a_0^{2 a_0} e^{2 a_1 + a_{18}}}{\pi a_0^2 a_8 a_9^2 a_{10}^{a_{10}} a_{13}^{a_{13}} a_{15}^{a_{15}} a_{18}^{a_{18}} \sqrt{a_{12} a_{14} a_{17} a_{19}} e^{a_4 + a_{11} + a_{16}}}$$
(81)

where

and

$$a_{20} = a_6^2 + (\eta\sqrt{n} + 2)a_6 - a_5^2 + a_5\eta\sqrt{n} + \eta\sqrt{n} - \sigma n/2 + 1/2.$$

Take the logarithm of F_n in equation (81) and expand. Expand the resulting expression asymptotically in n. Collect the leading order terms to obtain

$$\log F_n \simeq 4\sigma n \log 2 - (5\log n)/2 + 2\log 2 - \log \pi - 4\log \sigma + \log(\eta + \delta_1 + \delta_2) + \log(2\eta\delta_2 + \delta_1\delta_2 - \sigma) - \eta^2/\sigma - 2\eta\delta_1/\sigma - \delta_1^2/\sigma - \delta_2^2/\sigma.$$
(82)

Exponentiate and simplify the result. This shows that

$$F_n \simeq \frac{(\eta + \delta_1 + \delta_2)(2\,\eta\delta_2 + 2\,\delta_1\delta_2 - \sigma)}{\pi\sigma^4 n^{5/2}} \, 16^{\sigma n + 1/2} e^{-(\eta^2 + 2\,\eta\delta_1 + \delta_1^2 + \delta_2^2)/\sigma}. \tag{83}$$

The sum over k in equation (79) is now done by multiplying this by $A^{\eta\sqrt{n}}$ (where A=(a-1)) and then integrating for $\eta\in(0,\infty)$.

The asymptotic approximation of G_n is similarly obtained, and the result is

$$G_n \simeq \frac{(\eta + \delta_1 + \delta_2)(2\eta\delta_1 + 2\delta_1\delta_2 - \sigma)}{\pi\sigma^4 n^{5/2}} \ 16^{\sigma n + 1/2} e^{-(\eta^2 + 2\eta\delta_2 + \delta_1^2 + \delta_2^2)/\sigma}. \tag{84}$$

Notice that this is the same result as for F_n , but with δ_1 and δ_2 interchanged. Multiplying equation (83) by $A^{\eta\sqrt{n}}$ and integrating over $\eta \in (0, \infty)$ gives

$$\frac{(\sigma \delta_{2} n \log A + \sqrt{n}(\delta_{2}^{2} - \sigma)) \log A}{\sqrt{\pi \sigma^{5} n^{5}}} \times A^{-\delta_{1}\sqrt{n}} 16^{\sigma n} e^{(\sigma^{2} n (\log A)^{2} - 4\delta_{2}^{2})/4\sigma} \left(1 + \operatorname{erf} \left(\frac{\sigma \sqrt{n} \log A - 2\delta_{1}}{2\sqrt{\sigma}} \right) \right) + \frac{2 \delta_{2} \sigma \sqrt{n} \log A + 2 \delta_{1} \delta_{2} + 2 \delta_{2}^{2} - \sigma}{\pi \sigma^{3} n^{5/2}} 16^{\sigma n} e^{-(\delta_{1}^{2} + \delta_{2}^{2})/\sigma}.$$

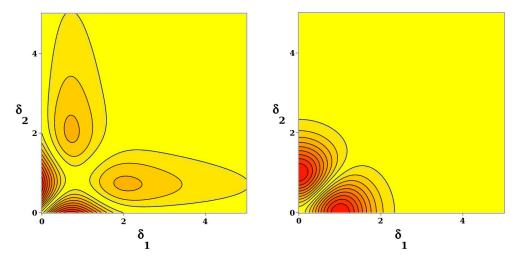


Figure 15: Contourplots of $|R_{2\lfloor \sigma n\rfloor}(2\lfloor \delta_1\sqrt{n}\rfloor, 2\lfloor \delta_2\sqrt{n}\rfloor)|$ on the $\delta_1\delta_2$ -plane. Low values are in light shades, and high values in darker shades. Left panel: The case that A=1.1 and n=25 while $\sigma=1.0$. This shows that paths with endpoints at heights $(\delta_1,\delta_2)\approx (0,1.4)$ or $(\delta_1,\delta_2)\approx (1.4,0)$ dominate the counts. There are secondary peaks at $(\delta_1,\delta_2)\approx (0.72,2.09)$ and (2.09,0.72). Right panel: The case that A=1 (at the adsorption critical point) and n=25 while $\sigma=1.0$. Paths with endpoints at heights $(\delta_1,\delta_2)\approx (0,1.0)$ or $(\delta_1,\delta_2)\approx (1.0,0)$ dominate the counts.

Expanding this asymptotically in n (and using equation (78)), keeping only leading order terms, and then simplifying produce

$$\sum_{k=0}^{n} F_n A^k \simeq \frac{2 \, \delta_2 (\log A)^2}{\sqrt{\pi \sigma^3 n^3}} \, 16^{\sigma n} A^{-\delta_1 \sqrt{n}} e^{\sigma n (\log A)^2 / 4} e^{-\delta_2^2 / \sigma}. \tag{85}$$

The similar result for G_n is

$$\sum_{k=0}^{n} G_n A^k \simeq \frac{2 \, \delta_1 (\log A)^2}{\sqrt{\pi \sigma^3 n^3}} \, 16^{\sigma n} A^{-\delta_2 \sqrt{n}} e^{\sigma n (\log A)^2 / 4} e^{-\delta_1^2 / \sigma}. \tag{86}$$

Denoting by $R_{2n}(h_1, h_2)$ the total number of states of half-length 2n, with endpoints of the paths at heights $h_1 = 2\lfloor \delta_1 \sqrt{n} \rfloor$ and $h_2 = 2\lfloor \delta_2 \sqrt{n} \rfloor$, then

$$R_{2\lfloor \sigma n \rfloor}(2\lfloor \delta_1 \sqrt{n}\rfloor, 2\lfloor \delta_2 \sqrt{n}\rfloor) \simeq \frac{2(\log A)^2}{\sqrt{\pi \sigma^3 n^3}} 16^{\sigma n} e^{\sigma n(\log A)^2/4} \times \left(\delta_2 A^{-\delta_1 \sqrt{n}} e^{-\delta_2^2/\sigma} - \delta_1 A^{-\delta_2 \sqrt{n}} e^{-\delta_1^2/\sigma}\right).$$

$$(87)$$

In figure 15 the absolute value $|R_{2\lfloor \sigma n\rfloor}(2\lfloor \delta_1\sqrt{n}\rfloor, 2\lfloor \delta_2\sqrt{n}\rfloor)|$ is plotted as a function of (δ_1, δ_2) . The peaks in the contour plot at $(\delta_1, \delta_2) \approx (0, 1.4)$ (or $(\delta_1, \delta_2) \approx (1.4, 0)$) corresponds to paths with $h_1 = 0$ and $h_2 \approx 2\lfloor 1.4\sqrt{n}\rfloor$ and this dominates the counts of pairs of paths. In this figure, n = 25, $\sigma = 1$ and A = 1.1. There are secondary peaks when $(\delta_1, \delta_2) \approx (0.72, 2.09)$ and (2.09, 0.72).

In the case that a=2 consider $r_{2n}(2j,2\ell)$ in equation (79) with $F_n(j,k,\ell)$ and $G_n(j,k,\ell)$ as given. Proceeding as above gives equations (83) and (84). In the case

that A = a - 1 = 1 the approximations of the sums F_n and G_n over n is obtained by integrated to η . This shows that to leading order

$$\sum_{k=0}^{n} F_n \simeq \frac{2(2\delta_1\delta_2 + 2\delta_2^2 - \sigma)}{\pi\sigma^3 n^{5/2}} 16^{\sigma n} e^{-(\delta_1^2 + \delta_2^2)/\sigma}, \tag{88}$$

$$\sum_{k=0}^{n} G_n \simeq \frac{2\left(2\delta_1^2 + 2\delta_1\delta_2^2 - \sigma\right)}{\pi\sigma^3 n^{5/2}} 16^{\sigma n} e^{-(\delta_1^2 + \delta_2^2)/\sigma}.$$
 (89)

In this event the approximation in equation (87) (for A = 1) becomes

$$R_{2[\sigma n]}(2[\delta_1\sqrt{n}], 2[\delta_2\sqrt{n}]) \simeq \frac{4(\delta_2^2 - \delta_1^2)}{\pi\sigma^3 n^{5/2}} 16^{\sigma n} e^{-(\delta_1^2 + \delta_2^2)/\sigma}.$$
 (90)

This is the approximation when a=2. In figure 13 the absolute value $|R_{2\lfloor \sigma n\rfloor}(2\lfloor \delta_1 \sqrt{n}\rfloor, 2\lfloor \delta_2 \sqrt{n}\rfloor)|$ is plotted in the right panel. Notice that the secondary peaks present in the left panel have disappeared but there are peaks at $(\delta_1, \delta_2) = (0, 1)$ and $(\delta_1, \delta_2) = (1, 0)$. This shows that paths with endpoints at heights $(h_1, h_2) = (0, \lfloor \sqrt{n} \rfloor)$ dominates the counts. In this figure n=25.

Data statement: No numerical data were generated in this study.

Acknowledgements: EJJvR is grateful for financial support from NSERC (Canada) in the form of a Discovery Grant RGPIN-2019-06303, and to York University for funds supporting this research.

References

- MT Batchelor and CM Yung. Exact results for the adsorption of a flexible self-avoiding polymer chain in two dimensions. Phys Rev Lett, 74:2026-2029, 1995.
- [2] M Bousquet-Mélou. Three osculating walkers. J Phys: Conf Ser, 42:35-47, 2006.
- [3] R Brak, JW Essam, and AL Owczarek. New results for directed vesicles and chains near an attractive wall. J Stat Phys, 93:155–192, 1998.
- [4] R Brak and AJ Guttmann. Exact solution of the staircase and row-convex polygon perimeter and area generating function. J Phys A: Math Gen, 23:4581–4588, 1990.
- [5] R Brak, AL Owczarek, A Rechnitzer, and SG Whittington. A directed walk model of a long chain polymer in a slit with attractive walls. J Phys A: Math Gen, 38:4309–4325, 2005.
- [6] MCTP Carvalho and V Privman. Directed walk models of polymers at interfaces. J Phys A: Math Gen, 21:L1033-L1037, 1988.
- [7] A Farb, PF Heller, S Shroff, L Cheng, FD Kolodgie, AJ Carter, DS Scott, J Froehlich, and R Virmani. Pathological analysis of local delivery of paclitaxel via a polymer-coated stent. *Circulation*, 104(4):473–479, 2001.
- [8] Gerard Fleer, MA Cohen Stuart, Jan MHM Scheutjens, T Cosgrove, and B Vincent. Polymers at interfaces. Springer Science & Business Media, 1993.
- [9] G Forgacs. Unbinding of semiflexible directed polymers in 1+1 dimensions. J Phys A: Math Gen, 24(18):L1099–L1103, 1991.
- [10] DP Foster. Exact evaluation of the collapse phase boundary for two-dimensional directed polymers. J Phys A: Math Gen, 23:L1135–L1138, 1990.
- [11] GK Iliev and EJ Janse van Rensburg. Directed path models of adsorbing and pulled copolymers. J Stat Mech: Theo Expr, 2012:P01019, 2012.
- [12] EJ Janse van Rensburg. Square lattice directed paths adsorbing on the line y=qx. J Stat Mech: Theo Expr, 2005:P09010, 2005.
- [13] EJ Janse van Rensburg. The adsorption transition in directed paths. J Stat Mech: Theo Expr, 2010:P08030, 2010.

- [14] EJ Janse van Rensburg. The statistical mechanics of interacting walks, polygons, animals and vesicles, 2nd ed. Oxford Lecture Series in Mathematics and its Applications. Oxford University Press, 2015.
- [15] EJ Janse van Rensburg. Trajectories of directed lattice paths. Physica Scripta, 98(3):035016, 2023.
- [16] EJ Janse van Rensburg and T Prellberg. The pressure exerted by adsorbing directed lattice paths and staircase polygons. J Phys A: Math Gen, 46:115202, 2013.
- [17] N Jawahar and SN Meyyanathan. Polymeric nanoparticles for drug delivery and targeting: A comprehensive review. Int J Health & Allied Sci, 1(4):217, 2012.
- [18] WB Liechty, DR Kryscio, BV Slaughter, and NA Peppas. Polymers for drug delivery systems. Ann Rev Chem Biomol Eng, 1:149, 2010.
- [19] KY Lin and WJ Tzeng. Perimeter and area generating functions of the staircase and row-convex polygons on the rectangular lattice. Int J Mod Phys B, 5:1913–1925, 1991.
- [20] DH Napper. Polymeric stabilization of colloidal dispersions, volume 3. Academic Press, 1983.
- [21] V Privman, G Forgacs, and HL Frisch. New solvable model of polymer-chain adsorption at a surface. Phys Rev B, 37:9897–9900, 1988.
- [22] A Rechnitzer and EJ Janse van Rensburg. Exchange relations, Dyck paths and copolymer adsorption. Disc Appl Math, 140:49-71, 2004.
- [23] Dirk Schmaljohann. Thermo-and pH-responsive polymers in drug delivery. Advanced drug delivery reviews, 58(15):1655–1670, 2006.
- [24] A Srivastava, T Yadav, S Sharma, A Nayak, AA Kumari, and N Mishra. Polymers in drug delivery. J Biosci Med, 4(1):69–84, 2015.
- [25] H Terayama, K Okumura, K Sakai, K Torigoe, and K Esumi. Aqueous dispersion behavior of drug particles by addition of surfactant and polymer. *Colloids and Surfaces B: Biointerfaces*, 20(1):73-77, 2001.
- [26] SG Whittington. A directed-walk model of copolymer adsorption. J Phys A: Math Gen, 31:8797–8803, 1998.